Elastic field of a surface step: Atomistic simulations and anisotropic elastic theory

L. E. Shilkrot and D. J. Srolovitz
Department of Materials Science and Engineering, University of Michigan, Ann Arbor, Michigan 48109-2136
(Received 27 November 1995)

Atomistic computer simulations and anisotropic elastic theory are employed to determine the elastic fields of surface steps and vicinal surfaces. The displacement field of and interaction energies between ⟨100⟩ steps on a {001} surface of Ni and Au are determined using atomistic simulations and embedded-atom method potentials. The step-step interaction energy found from the simulations is consistent with a surface line force dipole elastic model of a step. We derive an anisotropic form for the elastic field associated with a surface line force dipole using a two-dimensional surface Green tensor for a cubic elastic half-space within the Stroh formalism. Both the displacement fields and step-step interaction energy predicted by the theory are shown to be in excellent agreement with the simulations. The symmetry of the step displacement field is used to determine analytically the relative values of the components of the surface force dipole vector.

I. INTRODUCTION

The elastic fields of steps on surfaces play a key role in a number of important surface phenomena, including interactions between surface steps; interactions between impurities, adatoms, and steps; epitaxial growth; surface reconstruction; and crystal shape. The interaction between surface defects is caused by the elastic lattice distortions which can extend far into the bulk of the crystal. Unlike for topological defects, such as dislocations, where the Burger's vector alone determines the displacement field, there is no topological relationship that uniquely specifies the elastic field of a step in terms of its magnitude and orientation. Therefore, several computer simulations and experiments have been performed in order to understand the relation between steps and their elastic fields.[1–5] Within the last 15 years, several theoretical models for the elastic field of a step have been proposed based upon continuum elasticity and assumptions regarding the step.[6,7] In the present paper, we employ atomistic simulation techniques to investigate the elastic field associated with surface steps. We then derive an anisotropic elastic theory of step elasticity and fit the variables to the results of the atomistic simulations. In this way, we obtain a fully parametrized, consistent description of step elasticity.

Marchenko and Parshin[6] suggested that the elastic fields of surface steps can be described in terms of a traction distribution upon a flat surface. They argued that the source of these tractions is associated with the surface stress (tension). The discontinuity of the surface stress at the surface sets up a force moment along the surface step of magnitude proportional to the surface stress. Marchenko and Parshin argued that this force moment must be compensated for by a surface force dipole oriented perpendicular to the surface along the line of the surface step. Using this approach, they estimated the magnitude of this vertical force dipole to be the product of the surface energy γ and the step height b (more careful consideration given in the same article leads to replacing surface energy γ by surface stress τ). Using this model and working within isotropic elasticity, Marchenko and Parshin predicted that the interaction energy between two identical steps (per unit length of the step) is

$$E_{\rm int}=\frac{2(1-\nu^2)}{\pi E}\left[\xi^2+(\tau b)^2\right]\frac{1}{d_0^2}, \tag{1}$$

where τb is the magnitude of the vertical force dipole, ξ is the magnitude of the force dipole in the lateral direction (providing one exists), d_0 is the separation between two steps, and E and ν are the Young's modulus and Poisson's ratio of the crystal, respectively. This interaction is repulsive between like steps and decays quadratically with the reciprocal step separation.

Several additional attempts have been made to study step-step interactions theoretically[3,4,8] in order to understand the energetics of vicinal surfaces in terms of a periodic array of identical steps on flat high-symmetry surfaces. Atomistic simulations of vicinal surface energetics have been performed using different descriptions of atomic interactions. These simulations show that the interaction energy decays quadratically with the inverse interstep separation, as predicted by Marchenko and Parshin. While the general arguments presented above clearly lead to the correct functional form for the decay of the elastic field with distance from the step, these simulations did not carefully examine the elastic field of the steps. Nor did these simulations provide the key piece of information needed to parametrize the elastic theory fully for steps, namely the surface force dipole vector.

Modern electron microscopy techniques have made it possible to measure indirectly the displacement field created by a single step.[9] Recently Stewart, Pohland, and Gibson[10] analyzed the electron-diffraction data from a ⟨211⟩ step on Si {111} in terms of a multipole expansion of the surface tractions. Based upon these results, the authors argue that the leading-order term in the expansion is that associated with a surface force dipole; however, some discrepancies between the experimental results and the elastic theory remained.

In the present paper, we present atomistic simulation results for ⟨100⟩ steps on a nominally flat {001} surface of nickel and gold. By examining the elastic interactions between steps as a function of the interstep spacing, we obtain one estimate of the magnitude of the surface force dipole. Next, we perform a detailed analysis of the displacement field associated with a surface step. In order to analyze these

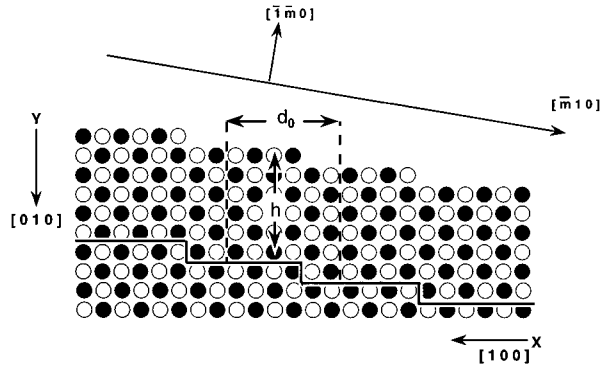

FIG. 1. The geometry of the simulation cell. Black and white circles denote atoms displaced in the Z direction by $a_0/2$, where a_0 is the perfect crystal lattice constant. This figure corresponds to a $(1\,\bar{6}0)$ surface. d_0 is the step separation and $b=a_0/2$ is the step height. The unit cell width is equal to the step separation, its height is h, and its thickness is a_0. Periodic boundary conditions are applied in the $[\bar{m}10]$ direction, and the atoms at $Y>h$ are frozen in their perfect crystal positions.

data in terms of an elastic model, we derive an anisotropic elastic theory for the elastic field of a step in terms of the surface force dipole vector. We then invert the surface step displacement field obtained from the simulation in order to determine the entire surface force dipole vector. The resultant dipole vector yields elastic step interaction energies in reasonable agreement with those obtained directly via atomistic simulation. Finally, an analysis of the elastic theory shows that the relative magnitudes of the components of the surface force dipole vector are determined simply by the anisotropic elastic constants of the crystal.

II. SIMULATION METHOD

In the present paper, we examine $[001]$ steps on the (010) surface of nickel and gold. In order to determine step-step interaction energies, we performed a series of simulations of several $(1\,\bar{m}0)$ vicinal surfaces. The geometry of the simulation cell and surface crystallography employed in the present study are shown in Fig. 1. In this figure, d_0 denotes the distance between two adjacent steps measured along the terrace in the direction perpendicular to the steps, and h is the height of the computational cell. The dimension of the computational cell in the direction in which the step runs is one face-centered-cubic lattice constant a_0 (which corresponds to two atomic layers), the separation between steps is in the range $8a_0 \leqslant d_0 \leqslant 80a_0$. Periodic boundary conditions were applied in both the Z direction (i.e., $[001]$) and in the $[\bar{m}10]$ direction.

The atomic interactions were described using embedded-atom-method (EAM) potentials.[11] In the this formalism the total energy $E_{\rm tot}$ consists of two distinct parts: a pairwise interaction energy and an on-site energy

$$E_{\rm tot}=\sum_{i=1}^{N}\sum_{j\neq i}\phi(r_{ij})+\sum_{i=1}^{N}F\left(\sum_{j\neq i}\rho(r_{ij})\right), \tag{2}$$

where N is the number of atoms in the system, r_{ij} is the separation between atoms i and j, and ϕ, ρ, and F are empirical functions fit to the universal binding energy relation and several experimentally determined parameters (elastic constants, lattice parameter, vacancy formation energy, etc.). The expressions for the empirical functions employed in the present simulations may be found in Ref. 12.

The equilibrium atomic structure and energy of the model were determined by minimizing the total energy with respect to the coordinates of all of the atoms using a conjugate gradient routine.[13] The simulation cell was matched to a perfect crystal lattice of the appropriate lattice parameter at a distance h below the free surface. During the course of the simulation, the height h of the computational cell was gradually increased until the total energy did not change to within an accuracy of 10^{-7} eV. The conjugate gradient method was deemed converged when the maximum force on any atom was less than or equal to 10^{-5} eV/a_0, and when the maximum atomic displacements in any one step were less than or equal to $10^{-6}\,a_0$.

In order to compare the interaction energies obtained in the present simulations with that predicted by Eq. (1), we calculated the surface stress tensor using the expression proposed in Ref. 14,

$$\boldsymbol{\tau}_{\alpha\beta}=-A_c^{-1}\sum_i\sum_k \mathbf{r}_{ki\beta}\mathbf{F}_{ki\alpha}. \tag{3}$$

Here $F_{ki\alpha}$ denotes the α component of the force on the ith site resulting from its interaction with site k, $\mathbf{r}_{ki\beta}$ is the β component of the radius vector from site i to site k, and A_c is the area of a unit cell of the surface. For a $\{010\}$ surface of a cubic material, the surface stress tensor is diagonal, i.e.,

$$\boldsymbol{\tau}_{\alpha\beta}=\tau\delta_{\alpha\beta}. \tag{4}$$

III. SIMULATION RESULTS

The step-step interaction energy $E_{\rm int}$ on $(\bar{1}\,\bar{m}0)$ vicinal surfaces of gold and nickel as a function of the square of the reciprocal interstep separation d_0^{-2} is shown in Figs. 2(a) and 2(b), respectively. Both sets of data show that over the range of interstep spacings considered here, the step-step interaction energy is well described by the d_0^{-2} functional form. This is consistent with the prediction of Eq. (1), and with earlier atomistic simulation results.[3,4] Earlier simulation results[4] suggest that at much smaller step spacings than considered here, higher-order terms in the step-step interaction energy dependence of the reciprocal interstep separation must also be included.

In order to evaluate the agreement of the simulation data with the functional form for $E_{\rm int}$ vs d_0 predicted by Eq. (1), we fit the data in Fig. 2 to the functional form

$$E_{\rm int}=\frac{A_1}{d_0}+\frac{A_2}{d_0^2}+\frac{A_3}{d_0^3}. \tag{5}$$

The step-step interaction energy is determined from the simulations as indicated in Ref. 4. If Eq. (5) provided a perfect fit to the entire range of simulation data, A_1 and A_3 would be exactly zero. Table I shows that A_1 is indeed very small for both Ni and Au. Although A_3 is nonzero, this term makes a negligible contribution to the interaction energy over the range of step spacings examined in the present

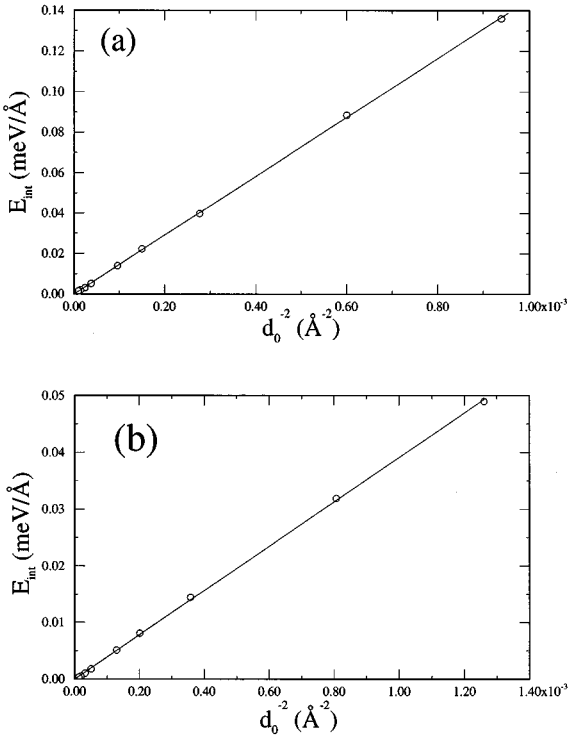

FIG. 2. Interaction energy of the steps on vicinal $(\bar{1}\,\bar{m}0)$ surfaces vs the square of the inverse step separation for (a) gold and (b) nickel.

study. The values for these A_m are similar to those obtained in a previous atomistic study of step-step interactions.[4]

The atomic displacement fields associated with individual [001] steps on the (010) surface of gold and nickel are shown in Figs. 3(a) and 3(b), respectively. These displacement fields were obtained from simulations in which the step separation was $d_0=80a_0$. In order to demonstrate that the step spacing was sufficiently large to guarantee that step-step interactions do not significantly modify the displacement fields, we also determined the displacement field for the same step in Ni, but with a step spacing $d_0=300a_0$ [see Fig. 3(c)]. The displacement fields for the steps separated by $d_0=80a_0$ and $300a_0$ are indistinguishable.

The maximum atomic displacements associated with the step are $1.9\times10^{-2}a_0$ in Ni, and $5.0\times10^{-2}a_0$ in Au. Excluding a region of radius $1a_0$ of the upper step edge, the maximum atomic displacements are $6\times10^{-3}a_0$ in Ni and $1.6\times10^{-2}a_0$ in Au. Since most of the remaining displacements are very small compared with the interatomic separation, we expect that linear elasticity should be applicable for describing the elastic field of the step (except, perhaps, within a very small region immediately surrounding the core of the step).

TABLE I. The coefficients of $(d_0)^{-m}$ in the expansion of the step-step interaction energy $E_{\rm int}$ vs the inverse interstep spacing d_0, as per Eq. (5).

	A_1 (eV)	A_2 (eV Å)	A_3 (eV Å^2)
Au	-0.0003 ± 0.0002	0.17 ± 0.02	-0.62 ± 0.34
Ni	$-0.000\,03\pm0.000\,02$	0.045 ± 0.001	-0.14 ± 0.02

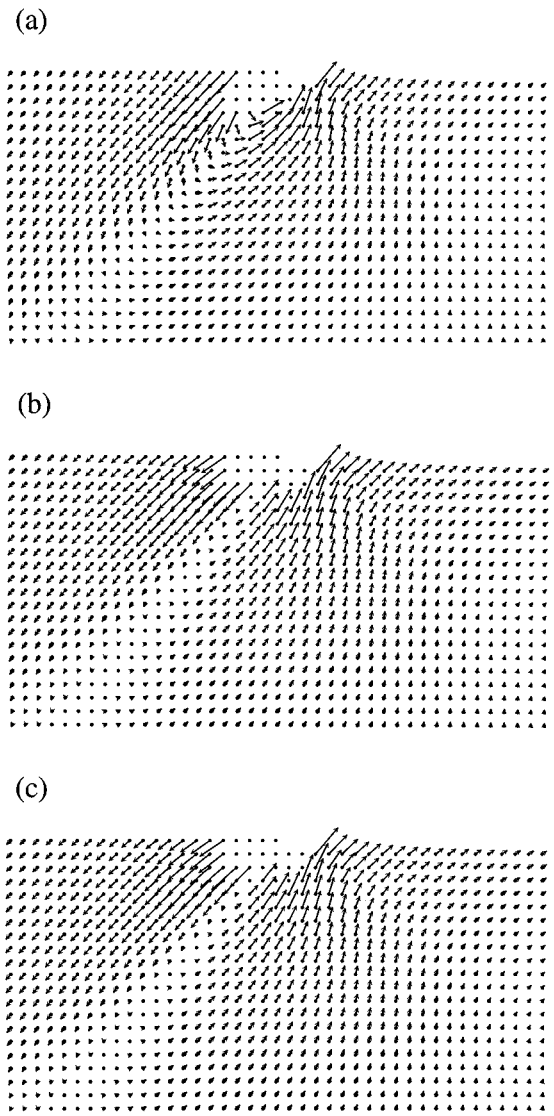

FIG. 3. Displacement field for a periodic array of ⟨100⟩ steps on a {001} surface obtained from the atomistic simulations. (a) and (b) correspond to gold and nickel surfaces, respectively, with a step separation $d_0=80a_0$ (only a segment of the surface is shown). (c) is the same as (b) except that $d_0=300a_0$. In order to improve the clarity, the atomic displacement vectors are magnified by a factor of 100 for gold and 200 for nickel. Displacements larger than $5\times10^{-3}a_0$, in the core region, are not shown.

The displacement fields associated with the steps in Au and Ni [Figs. 3(a) and 3(b)] are very similar. They are characterized by decreasing magnitude with distance from the step. In both cases, there is a plane, canted with respect to the vertical, across which the out-of-plane displacements change sign. The in-plane displacements also change sign as the same plane is crossed. Therefore, in both the Au and Ni cases, the step displacement fields exhibit a plane of zero (or nearly zero) displacement which is canted toward the upper side of the step. The fact that this plane is canted with respect to the surface normal is unexpected, since the simplest model of a surface step (based upon Marchenko and Parshin's surface stress argument) implies a surface force dipole oriented perpendicular to the nominal surface.

Although it is possible to analyze the displacement field

associated with the surface step (determined from the simulations) in terms of an isotropic elastic surface force dipole vector model, such an analysis would be inappropriate because the elastic anisotropy in nickel is substantial. One of the effects of this anisotropy can be seen in Fig. 3. If both the Au and Ni were isotropic, then the step displacement fields in these two materials would be identical with the possible exception of an overall scale factor. Careful examination of Figs. 3(a) and 3(b) show that the planes about which the displacements change signs occur at different angles in these two materials. Therefore, an anisotropic elastic analysis of the displacement fields of the step is necessary.

IV. ELASTIC ANALYSIS

Consider the case of a step oriented parallel to the OZ direction on a surface with normal OY. The direction OX lies within the surface, perpendicular to the direction in which the step runs. The step is at the origin of the coordinate system. Further, let the material occupy the half-space $y>0$. The displacement field associated with any distribution of surface tractions can be written as a convolution of these tractions $\mathbf{T}(x,z)$ with the elastic surface Green tensor $\mathbf{G}(x,y,z)$:

$$\mathbf{u}(x,y,z)=\int dS\ \mathbf{G}(x-x',y,z-z')\mathbf{T}(x',z'). \tag{6}$$

In the straight surface step case, the problem is strictly two dimensional, since the surface tractions are assumed to be uniform along the step line, i.e., they are independent of the coordinate along a step. These tractions will be denoted as $\mathbf{T}(x)$. The Green tensor $\mathbf{G}(x,y,z)$ can, therefore, be integrated along the step direction to yield $\mathbf{G}(x,y)$.

In Marchenko and Parshin's model, the tractions produced by a step are assumed to be associated with a surface line force dipole which, in the most general case, may be tilted with respect to the surface,

$$\mathbf{T}(x)=\mathbf{D}\delta'(x), \tag{7}$$

where δ' is a derivative of a delta function, and $\mathbf{D}$ is the surface force dipole vector. The resultant expression for the displacement field associated with a single surface step is simply [inserting Eq. (7) into Eq. (6)]

$$\mathbf{u}(x,y)=\mathbf{g}(x,y)\mathbf{D}, \tag{8}$$

where $\mathbf{g}(x,y)$ is a 3×3 matrix,

$$\mathbf{g}(x,y)=-\frac{\partial}{\partial x}\mathbf{G}(x,y). \tag{9}$$

The tensor $\mathbf{g}$ is easily obtained for the case of an isotropic medium[10] from the well-known isotropic elastic surface Green tensor $\mathbf{G}(x,y,z)$.[15] For our purposes, the main feature of this tensor is that (in polar coordinates) each of its components can be factored as a product of an angular part $\mathbf{f}_{ij}(\theta)$ and a radial part which is proportional to $1/r$, where r is the distance from the origin. The off-diagonal elements of the matrix $\mathbf{f}$ vanish at the surface and exhibit the following symmetry:

$$\mathbf{f}_{xy}=-\mathbf{f}_{yx}. \tag{10}$$

For an anisotropic medium, an analytical expression for $\mathbf{G}$ can be obtained only for the case of hexagonal symmetry.[16] However, for two-dimensional problems, the complexity of the problem can be significantly reduced by using the formalism developed by Stroh.[17] The expression for the derivative of the surface Green tensor $\mathbf{g}$, derived in this way, is presented in the Appendix. For the case of a step oriented along $\langle001\rangle$ on a $\{001\}$ surface of a cubic crystal, an expression for $\mathbf{g}$ can be found analytically in closed form. The elements of the derivatives of the surface Green tensor $\mathbf{g}$ in polar coordinates are

$$\mathbf{g}=\begin{pmatrix} \frac{1}{r}\frac{\mathbf{f}_{xx}(\theta)}{\pi L d(\theta)} & \frac{1}{r}\frac{\mathbf{f}_{xy}(\theta)}{\pi L d(\theta)} \\ \frac{1}{r}\frac{\mathbf{f}_{yx}(\theta)}{\pi L d(\theta)} & \frac{1}{r}\frac{\mathbf{f}_{yy}(\theta)}{\pi L d(\theta)} \end{pmatrix}, \tag{11}$$

where

$$\begin{aligned} \mathbf{f}_{xx}(\theta)&=C_{44}\cos(\theta)[C_{12}\cos^2(\theta)-C_{11}\sin^2(\theta)],\\ \mathbf{f}_{xy}(\theta)&=C_{44}\sin(\theta)[C_{12}\sin^2(\theta)-C_{11}\cos^2(\theta)],\\ \mathbf{f}_{yx}(\theta)&=C_{44}\sin(\theta)[C_{11}\sin^2(\theta)-C_{12}\cos^2(\theta)], \end{aligned} \tag{12a}$$

$$\begin{aligned} \mathbf{f}_{yy}(\theta)=\cos(\theta)\{&H\cos^2(\theta)(C_{11}+C_{12})+C_{12}C_{44}\\ &+(C_{11}+C_{12})[C_{11}-C_{12}+C_{44}\cos^2(\theta)]\}, \end{aligned}$$

$$d(\theta)=H(C_{11}+C_{12})\cos^2(\theta)\sin^2(\theta)+C_{11}C_{44}, \tag{12b}$$

and

$$L=\frac{C_{44}(C_{11}-C_{12})}{\sqrt{\left(4\frac{C_{11}C_{44}}{C_{11}+C_{12}}+H\right)\left(\frac{C_{11}C_{44}}{C_{11}+C_{12}}\right)}}. \tag{12c}$$

H is the elastic anisotropy of the cubic crystal: $H=C_{11}-C_{12}-2C_{44}$, and C_{11}, C_{12}, and C_{44} are the three unique elastic constants of a cubic crystal. The form of Eqs. (11) and (12) preserve the same structure of the derivative of the Green tensor found in the isotropic case: the radial parts are all proportional to $1/r$. The angle θ is measured from the OX axis to the OY axis in a counterclockwise manner (see Fig. 1). All elements of the tensor $\mathbf{g}$ in which one of the indices is z are identically zero except for $\mathbf{g}_{zz}$. However, because of the symmetry of the surface step problem, the magnitude of the dipole force in the OZ direction is zero.

Given the green tensor $\mathbf{g}$, the interaction energy between two identical steps E_2 can be readily obtained from the general expression for the elastic interaction energy between two surface loads:

$$E_{\rm int}=\int dS\ \mathbf{T}_1(x,z)\mathbf{u}_2(x,z), \tag{13}$$

where $\mathbf{T}_1(x,z)$ is the traction associated with the first load, $\mathbf{u}_2(x,z)$ is the displacement vector associated with the tractions of the second load, and the integral is evaluated over the entire surface. Inserting Eqs. (7) and (8) into Eq. (13) yields

$$E_2 = \frac{\mathbf{DD}}{\pi L d_0^2} = \frac{\mathbf{D}_x^2 + \mathbf{D}_y^2}{\pi L d_0^2}. \tag{14}$$

The interaction energy of a periodic array of parallel, identical steps was derived in Ref. 4 and is given by

$$E_{\text{int}} = \frac{\pi^2}{6} E_2 = \frac{\pi}{6} \frac{\mathbf{D}_x^2 + \mathbf{D}_y^2}{L d_0^2}. \tag{15}$$

This result is the anisotropic generalization of the isotropic result of Marchenko and Parshin[6] presented in Eq. (1), for the case of a ⟨100⟩ step on a {001} surface of a cubic crystal. Like the isotropic theory and the simulation results, this interaction energy decays with step spacing as d_0^{-2}. In terms of the expansion of the step-step interaction energy data for the vicinal surface in terms of the inverse step spacing, the parameter A_2 in Eq. (5) is

$$A_2 = \frac{\pi}{6} \frac{\mathbf{D}_x^2 + \mathbf{D}_y^2}{L}. \tag{16}$$

The only unspecified parameters in this analysis are $\mathbf{D}_x$ and $\mathbf{D}_y$ which, together, specify the orientation of the surface line force dipole. Comparison of Eq. (16) with the simulated elastic step-step interaction energy data from the simulation (presented in Table I) allows direct determination of $\mathbf{D}_x^2 + \mathbf{D}_y^2$. The individual components of the surface line force dipole vector may be extracted directly from the displacement field determined in the atomistic simulations. Both of these analyses are performed below.

V. DISCUSSION

The simulation results presented above suggest that the leading-order term in the expansion of the step-step interaction energy in a series of reciprocal powers of distance is quadratic, i.e., d_0^{-2}. This is consistent with the predictions of both the isotropic and our anisotropic elastic theories that model the elastic field of a step in terms of a surface line force dipole. Nonzero higher-order terms in this expansion may be associated with surface force distributions which contain quadrupole or higher-order terms. The next-order term in the expansion of the step-step interaction energy d_0^{-3} is associated with the interaction between a dipole on one step and a quadrapole on another step.[18] The relative contribution of this third-order term can be estimated in terms of a dimensionless parameter

$$K = \left| \frac{A_3}{d_0 A_2} \right|. \tag{17}$$

For $K < 0.2$, the third-order term makes less than a 20% correction to the step-step interaction energy. Using the simulation data in Table I, this only occurs for step spacings bigger than approximately 18 Å in Ni and Au (i.e., >5 lattice parameters). Although it is not possible to extract the surface line dipole force vector (or its magnitude) from elastic theories, comparison of atomistic simulation and elastic theory results can be employed uniquely to determine this dipole force vector.

The most direct method for extracting the surface line force dipole vector from the atomistic simulations is by direct comparison of the displacements determined via the simulation with the analytical, anisotropic form of Eqs. (8)–(12). The two independent components of the surface line force dipole vector $\mathbf{D}_x$ and $\mathbf{D}_y$ were chosen to provide the best fit to the displacement field obtained from the simulations using a least-squares fitting procedure. There is ambiguity on the scale of an interatomic spacing as to which line on the surface to associate with the step location. We arbitrarily assumed that the step is located at the upper edge of the step (i.e., at the edge of the upper terrace). In order to exclude the effect of surface relaxation, we excluded all atoms within the three (020) planes closest to the surface from the fit. Similarly, to eliminate the effects of nonlinear elastic displacements near the ''core'' of the step, we also excluded all atoms that were within a radius of four atomic spacings of the step from the fit. The best-fit, anisotropic elastic displacement field associated with a surface line force dipole is shown in Figs. 4(a) and 4(b) for the case of an [001]-oriented step on a (010) surface in gold and nickel, respectively. Comparison of Figs. 3 and 4 shows that the theoretical predictions of the displacement fields are in excellent agreement with the atomistic data for both nickel and gold everywhere, except for some small differences very near the step itself. It is also possible to invert the Green tensor for the surface line dipole Eq. (9) locally, at each atomic position, and investigate the variation of the surface line force dipole needed to produce those local displacements and the magnitude of the parameter A_2 in the step-step interaction energy obtained

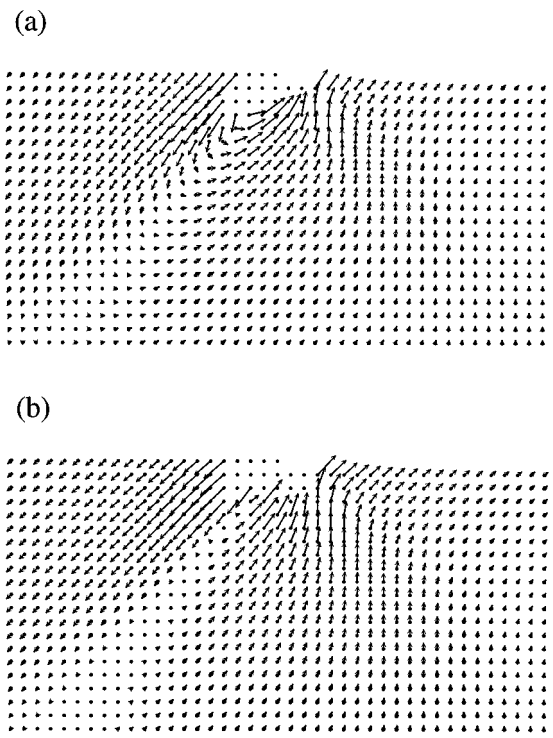

FIG. 4. Displacement field for a periodic array of ⟨100⟩ steps on a {001} surface obtained from the anisotropic elastic theory [Eq. (8)] using the best-fit surface line force dipole vector **D**. (a) and (b) correspond to gold and nickel surfaces, respectively, with a step separation $d_0 = 80a_0$ (only a segment of the surface is shown). The magnification factors used for the displacements are exactly as shown in Fig. 3.

TABLE II. The two independent components of the surface line force dipole $\mathbf{D}_x$ and $\mathbf{D}_y$ (eV/Å) and the coefficient A_2 (eV Å) of $(d_0)^{-2}$ in the expansion of the step-step interaction energy E_{int} vs the inverse interstep spacing d_0, as per Eq. (5) with $A_1=A_3=0$ (as discussed in the text). Table II(a) presents data for Au, and Table II(b) presents data for Ni. The ''Theory (fit)'' data were obtained from a least-square fit of Eq. (8) to the simulation data. The value of A_2 in the row labeled ''Simulations'' was determined from Fig. 2. The data in the rows labeled ''τb'' and ''γb'' were obtained using Eqs. (8) and (16) and the values of the surface stress and surface energy determined in the present simulations. $b=a_0/2$ is the surface step height.

(a)

Au	$\mathbf{D}_x$	$\mathbf{D}_y$	A_2
Simulations			0.15
Theory (fit)	0.17	0.18	0.13
τb		0.40	0.34
γb		0.12	0.03

(b)

Ni	$\mathbf{D}_x$	$\mathbf{D}_y$	A_2
Simulations			0.039
Theory (fit)	0.15	0.13	0.033
τb		0.29	0.070
γb		0.17	0.025

from Eq. (16). For all but a small number of points, this procedure produces only small variations in the surface line force dipole values and the step-step interaction energy coefficient A_2. This further demonstrates the accuracy and consistency between the anisotropic elastic analytical predictions of the step elastic field and that found from our atomistic simulations.

The core of the step is the region near the step in which the linear elastic theory fails to describe the atomic displacement field accurately. Although this definition of core size depends on the threshold we use to determine whether the displacement fields are sufficiently accurately reproduced by linear elasticity, we can make a reasonable choice, such that small changes in this threshold do not significantly change change the core size. Using the best-fit values of $\mathbf{D}_x$ and $\mathbf{D}_y$ and a threshold error of 10%, we estimate the step core radius to be approximately $3a_0$ for these steps in both Ni and Au.

Table II shows the values of $\mathbf{D}_x$ and $\mathbf{D}_y$ obtained by fitting Eq. (8) to the displacement field found from the atomistic simulations. In order to establish the consistency of these results with respect to the simulations, Table II compares the magnitude of the step-step interaction energies (A_2) obtained by varying the step spacing in the simulations directly with the predictions of the analytical theory, Eq. (16). The resultant values agree to within 15% for both Au and Ni. We note that an error of order $+\varepsilon$ in $\mathbf{D}_x$ and $\mathbf{D}_y$ leads to an error of up to 4ε in A_2. Therefore, we conclude that the errors in $\mathbf{D}_x$ and $\mathbf{D}_y$ are in the range of 4–15 %. On this basis, we conclude that the analytical anisotropic elastic theory is in excellent agreement with the simulations.

In Marchenko and Parshin's[6] original paper on step-step interactions, they speculated that the magnitude of the line force dipole oriented normal to the surface is equal to the product of the surface stress and the step height, i.e., τb. In order to examine this assertion, we have calculated the surface stress for the {001} surface of Ni and Au. The data are tabulated in Table III, along with the {001} surface energy determined from the simulation and polycrystalline average surface energies determined experimentally. The surface stress is found to be 1–4 times larger than the surface energy. Hence approximating one with the other would be a poor approximation. Additionally, the computed surface energies are significantly smaller than the experimental values. This is due in large part to the fact that the EAM potentials routinely underestimate the surface energies of fcc metals, and that the experimental values are polycrystalline averages. Inserting the surface stress values determined from these simulations into the expression for the step-step interaction energy parameter for the vicinal surface [A_2 in Eq. (16)], we find that Marchenko and Parshin's speculation that the magnitude of the surface line force dipole is equal to the product of the surface stress and the step height yields results that are of the correct order of magnitude. However, only including the τb term in A_2 ignores the possibility of a force dipole in the plane of the surface [see Eq. (1) above]. Such a term would only further increase Marchenko and Parshin's predicted value of A_2, which is already too large by approximately 100% compared with the simulation results.

TABLE III. The surfaces stress τ and surface energy γ of the {001} surface of Au and Ni determined from the present atomistic simulations. For comparison, we also enclose the surface energy determined from experiments using polycrystalline samples $\overline{\gamma}_{\text{exp}}$ (Ref. 20).

	τ (eV/Å^2)	γ (eV/Å^2)	$\overline{\gamma}_{\text{exp}}$ (eV/Å^2)
Au	0.196	0.057	0.094
Ni	0.164	0.098	0.149

Both the displacement fields obtained from the atomistic simulations and those determined using Eq. (8) (see Figs. 3 and 4) show that a plane exists along which the atomic displacements are very nearly zero. This plane passes through the step and hence occurs at some angle, which we label θ_0. Analytically, the occurrence of such a zero displacement plane at θ_0 implies that the following condition must be satisfied:

$$\mathbf{g}(\theta_0)\mathbf{D}=\mathbf{0}. \tag{18}$$

This can only occur if the determinant of $\mathbf{g}$ at θ_0 is identically zero. For the step geometry considered here (i.e., $\langle 100\rangle$ steps on a {001} surface), this implies that θ_0 must satisfy the following condition:

$$\tan^2\theta_0=\frac{C_{11}}{C_{12}}. \tag{19}$$

Therefore, the angle of the zero displacement plane is simply a function of the elastic constants. Equation (19) is a necessary condition in order to satisfy Eq. (18), but not a sufficient one. Using the value of θ_0 determined in Eq. (19), we find that Eq. (18) is satisfied only if the two components of the surface line force dipole vector satisfy the following relation:

$$\frac{\mathbf{D}_y}{\mathbf{D}_x} = \frac{C_{44}}{\sqrt{C_{11}C_{12}}}. \tag{20}$$

Equation (20) implies that the ratio of the two components of the surface line force dipole vector is determined solely by the elastic constants of the material.

Ni and Au have much different elastic anisotropies—$H(\mathrm{Au}) = -0.40$ eV/Å^3 and $H(\mathrm{Ni}) = -1.10$ eV/Å^3 using the elastic constants derived from the EAM potentials. However, these anisotropies produce only a relatively small difference in θ_0: $\theta_0(\mathrm{Au}) = 47.0°$ and $\theta_0(\mathrm{Ni}) = 50.9°$. θ_0 can also be extracted from the displacement fields shown in Fig. 3, which were determined from the atomistic simulations. These values determined from the simulations are $\theta_0(\mathrm{Au}) = 50° \pm 3°$ and $\theta_0(\mathrm{Ni}) = 51° \pm 2°$. The values of θ_0 determined from the elastic constants [Eq. (19)] are within the error bars of those obtained from the simulations. Although the predicted values for θ_0 for Au and Ni are very similar, the values determined from the simulations are such that $\theta_0(\mathrm{Au}) < \theta_0(\mathrm{Ni})$, in agreement with the theoretical predictions. The predicted angles could be better tested in a material such as diamond where the anisotropy is very large: $\theta_0(\mathrm{diamond}) = 71°$.

VI. CONCLUSIONS

Atomistic computer simulation and anisotropic elastic theory were applied to the determination of the elastic fields of individual surface steps and steps on vicinal surfaces. The displacement field of and interaction energies between ⟨100⟩ steps on a {001} surface of Ni and Au were determined using zero-temperature atomistic simulations and embedded-atom-method interatomic potentials. A fit of the step-step interaction energy determined from simulations in terms of a power law in the inverse step spacing shows that the leading order term in the step-step interaction energy is proportional to the inverse square of the step spacing. This is consistent with a surface line force dipole elastic model of a step. In order to fit the simulation data to the elastic model, we derived an anisotropic form for the elastic field associated with a surface line force dipole using a two-dimensional surface Green tensor for a cubic elastic half-space within the Stroh formalism. This is necessary since Ni has a large elastic anisotropy. One input into the analytical description of the elastic fields of the step is the surface force dipole vector associated with the step. We determined this dipole vector by fitting the displacement field determined from the simulation with the results of the anisotropic elastic theory. We demonstrated that this fit is excellent for both Ni and Au. This dipole vector was combined with the anisotropic elastic theory to predict the step-step interaction energy. This too was shown to be in excellent agreement with the simulations. Finally, the symmetry of the displacement field associated with the step suggests an analytical method for determining the relative values of the components of the surface force dipole vector in terms of the anisotropic elastic constants. This reduces the determination of the elastic field of a step to a single parameter.

ACKNOWLEDGMENTS

The authors would like to thank Professor J. Barber, Professor D. Barnett, and Dr. R. Najafabadi for useful discussions. Further, the authors gratefully acknowledge the Division of Materials Science of the Office of Basic Energy Sciences of the United States Department of Energy, Grant No. FG02-88ER45367 for its support of this work.

APPENDIX: ANISOTROPIC SURFACE ELASTIC GREEN TENSOR

The elastic Green tensor associated with an isotropic elastic half-space is easily derived and is well known.[15] While the Green tensor for an anisotropic half-space may also be determined, it cannot be evaluated analytically except in special cases, e.g., a hexagonal crystal.[16] Fortunately, this complexity may be significantly reduced in two-dimensional problems by application of the Stroh formalism.[17]

Let us consider an anisotropic, elastic half-space occupying the region $y > 0$, with the x axis parallel to the surface. This problem is two dimensional, and all solutions are independent of the coordinate z. Following the approach proposed by Ting,[19] we introduce the following 3×3 matrices:

$$Q_{ik}(\theta) = C_{ijks} n_j n_s, \quad R_{ik}(\theta) = C_{ijks} n_j m_s,$$
$$T_{ik}(\theta) = C_{ijks} m_j m_s, \tag{A1}$$

where $n_i = [\cos\theta, \sin\theta, 0]$, $m_i = [-\sin\theta, \cos\theta, 0]$, and C_{ijrs} is the anisotropic elastic constant tensor. The angle θ is measured with respect to the OX axis in a counterclockwise direction (i.e., towards the OY axis). It is useful to identify the following three matrices:

$$\mathbf{N}_1(\theta) = -\mathbf{T}^{-1}(\theta)\mathbf{R}^T(\theta), \quad \mathbf{N}_2(\theta) = \mathbf{T}^{-1}(\theta),$$
$$\mathbf{N}_3(\theta) = \mathbf{R}(\theta)\mathbf{T}^{-1}(\theta)\mathbf{R}^T(\theta) - \mathbf{Q}(\theta), \tag{A2}$$

and three incomplete integrals

$$\mathbf{S}(\theta) = \frac{1}{\pi}\int_0^\theta N_1(\omega)\,d\omega, \quad \mathbf{H}(\theta) = \frac{1}{\pi}\int_0^\theta \mathbf{N}_2(\omega)\,d\omega,$$
$$\mathbf{L}(\theta) = -\frac{1}{\pi}\int_0^\theta \mathbf{N}_3(\omega)\,d\omega. \tag{A3}$$

The surface Green tensor $\mathbf{G}_{ij}(r,\theta)$ for an anisotropic, elastic half-space may now be written in terms of these quantities as [see expression (5.2) in the same article[19]]:

$$\mathbf{G} = -\left[\frac{1}{\pi}(\ln r)\mathbf{I} + \mathbf{S}(\theta) - \frac{1}{2}\mathbf{S}\right]\mathbf{L}^{-1}, \tag{A4}$$

where $\mathbf{I}$ is an identity matrix, and

$$\mathbf{S} = \mathbf{S}(\pi), \quad \mathbf{H} = \mathbf{H}(\pi), \quad \mathbf{L} = \mathbf{L}(\pi). \tag{A5}$$

Integrals (A3) and (A5) can be computed analytically only in a few special cases. However, in order to describe the

displacement field associated with a surface force line dipole, we need only evaluate the derivative of the surface Green's function with respect to x, rather than the entire surface Green tensor itself. This simplification allows us to avoid evaluating the indefinite integrals Eq. (A3) altogether, and only the elements of the matrix **L**, which are the definite integrals Eq. (A5), need to be computed. At most, the matrix **L** contains six unique elements because it is symmetric. The resultant expression for the surface dipole Green tensor **g** is

$$\mathbf{g}=-\frac{\partial}{\partial x}\mathbf{G}=\frac{1}{r}\left[\mathbf{I}\cos\theta-\mathbf{N}_1\sin\theta\right]\mathbf{L}^{-1}. \tag{A6}$$

In the case of cubic symmetry, when the half-space is bounded by a {001}-type plane and the ⟨100⟩ step lies along OZ (as in the present case), this problem can be solved analytically. The matrix **L** becomes diagonal:

$$\mathbf{L}_{33}=C_{44}, \tag{A7}$$

$$\mathbf{L}_{11}=\mathbf{L}_{22}=L=\frac{C_{44}(C_{11}-C_{12})}{\left[\left(4\dfrac{C_{11}C_{44}}{C_{11}+C_{12}}+H\right)\left(\dfrac{C_{11}C_{44}}{C_{11}+C_{12}}\right)\right]^{1/2}},$$

where H is the crystal anisotropy, $H=C_{11}-C_{12}-2C_{44}$. In the isotropic limit ($H\to 0$), Eq. (A6) reduces to the well-known isotropic elastic surface dipole Green tensor.[10]

If we examine {111} surfaces rather than the {001} surfaces, as in recent experiments, computation of the elements of **L** requires either solving a cubic equation or numerical evaluation. Except for this step, the procedure for deriving the surface Green tensor for a {111} surface is essentially the same as that outlined above for the {010}-[001] surface step geometry.

[1] P. Wynblatt, in *Interatomic Potentials and Simulation of Lattice Defects*, edited by P. Gehlen, J. R. Beeler, Jr., and R. I. Jaffee (Plenum, New York, 1972).

[2] Tze Wing Poon *et al.*, Phys. Rev. Lett. **65**, 2161 (1990).

[3] D. Wolf and J. A. Jaszczak, Surf. Sci. **277**, 301 (1992).

[4] R. Najafabadi and D. J. Srolovitz, Surf. Sci. **317**, 221 (1994).

[5] S. Kodiyalam *et al.*, Phys. Rev. B **51**, 5200 (1995).

[6] V. I. Marchenko and A. Ya. Parshin, Zh. Eksp. Teor. Fiz. **79**, 257 (1980) [Sov. Phys. JETP **52**, 129 (1980)].

[7] D. J. Srolovitz and J. P. Hirth, Surf. Sci. **255**, 111 (1991).

[8] B. Houchmandzadeh and C. Misbah, J. Phys. (France) I **5**, 685 (1995).

[9] O. Pohland, X. Tong, and J. M. Gibson, J. Vac. Sci. Technol. A **11**, 1837 (1993).

[10] J. Stewart, O. Pohland, and J. M. Gibson, Phys. Rev. B **49**, 13 848 (1994).

[11] M. S. Daw and M. I. Baskes, Phys. Rev. B **29**, 6443 (1984).

[12] S. M. Foiles, M. I. Baskes, and M. S. Daw, Phys. Rev. B **33**, 7983 (1986).

[13] W. H. Press *et al.*, *Numerical Recipes in C: The Art of Scientific Computing*, 2nd ed. (Cambridge University Press, New York, 1992), pp. 420–425.

[14] G. J. Ackland and M. W. Finnis, Philos. Mag. A **54**, 301 (1986).

[15] L. D. Landau and E. M. Lifshitz, *Theory of Elasticity*, 3rd ed. (Pergamon, Oxford, 1986).

[16] I. M. Lifshitz and L. N. Rozentsveig, Zh. Eksp. Teor. Fiz. **17**, 783 (1947).

[17] A. N. Stroh, Philos. Mag. **3**, 625 (1958).

[18] J. M. Rickman and D. J. Srolovitz, Surf. Sci. **284**, 211 (1993).

[19] T. C. T. Ting, Q. J. Mech. Appl. Math. **45**, 119 (1992).

[20] W. R. Tyson and W. A. Miller, Surf. Sci. **62**, 267 (1977).